Current and shot noise measurements in a carbon nanotube-based spin diode (invited)

Christopher A. Merchant and Nina Marković[a)]
Department of Physics and Astronomy, Johns Hopkins University Baltimore, Maryland 21218, USA

(Presented 11 November 2008; received 18 September 2008; accepted 16 November 2008; published online 20 March 2009)

Low-temperature measurements of asymmetric carbon nanotube (CNT) quantum dots are reported. The CNTs are end-contacted with one ferromagnetic and one normal-metal electrode. The measurements show a spin-dependent rectification of the current caused by the asymmetry of the device. This rectification occurs for gate voltages for which the normal-metal lead is resonant with a level of the quantum dot. At the gate voltages at which the current is at the maximum current, a significant decrease in the current shot noise is observed. © *2009 American Institute of Physics*. [DOI: 10.1063/1.3072020]

Carbon nanotubes (CNTs) (Ref. 1) are ballistic conductors that have long mean-free paths and spin diffusion lengths.[2,3] CNTs can therefore be used as spacers for spin valves[4–6] or in other systems that require spin coherence over their lengths.[7] Additionally, short CNT sections behave like quantum dots at low temperatures.[8] Short CNT sections are therefore promising materials for charge detection,[9] the separation of spin-entangled pairs of electrons,[10,11] or the rectification of current based on the electron spin.[12,13] Recently spin-based current rectification, or a spin diode effect,[13–18] has been observed in a lateral ferromagnet-CNT-normal-metal device.[19] Shot noise measurements can provide an additional window into the dynamics of a system.[20] Noise measurements are useful for examining the correlation of tunneling events in a system, and have been studied for double-barrier tunnel junctions.[21–23] Here we extend upon previous results by considering the current noise of a CNT-based spin diode.

A schematic of our device is given in Fig. 1(a). It consists of a single-walled carbon nanotube (SWNT) grown by chemical vapor deposition[24] and end-contacted to alternating niobium and cobalt electrodes. Devices are measured by applying a bias voltage and a capacitively coupled gate voltage and measuring the two-terminal current. A representative atomic force microscopy (AFM) image of a device is shown in Fig. 1(b). We have also measured the resistance of sections of the niobium electrode as a function of temperature, which is shown in Fig. 1(c). We observe that there the resistance drops to zero around 6.5 K as the niobium electrode becomes superconducting.

Electronic transport measurements were performed at temperatures ranging from 4.2 to 10 K. Figures 2(a) and 2(b) show conductance measurements at both the high- and low-temperature extremes, respectively. We observe typical Coulomb blockade behavior at both temperatures.[25] From the conductance maps we are able to determine the ratio of capacitances, α, for the single electron transistor (SET).[26] We measure $\alpha = C_G / C_{\text{tot}} \sim 0.02$ for this sample, which is similar to other samples we have measured. We also find that at temperatures below the measured value of T_c, as in Fig. 2(b), an additional energy gap of ~ 1 meV opens up, stretching the low-conductance region in the bias direction. The energy value of this extra gap corresponds to 2Δ based on our measurements of T_c of the niobium electrode, where Δ is the superconducting energy gap.[27] This compares to a previous measured gap of 2Δ in quantum dots connected to one superconducting and normal-metal lead[28] and 4Δ for two superconducting leads.[29]

Figures 3(a) and 3(b) give the conductance as a function of bias voltage and gate voltage at 10 and 4.2 K, respectively. We have focused on a range of the gate voltage where the total coulomb blockade values $(U+\Delta E)$ are all about the same. This indicates that the spin degeneracy of the energy levels of the quantum dot has been broken.[30] The additional

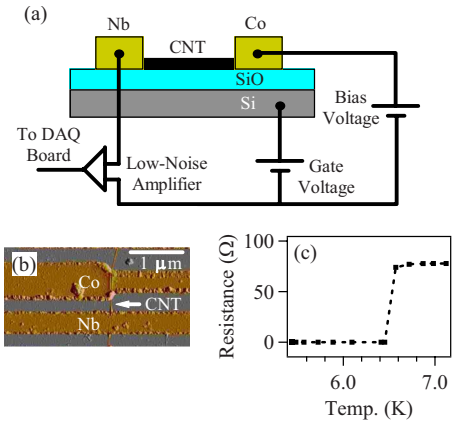

FIG. 1. (Color online) (a) Schematic of the measurement setup. Bias is applied between the niobium and the cobalt lead with niobium lead grounded. Gate voltage is applied to the doped silicon substrate through a 500 nm thick thermally grown layer of SiO_2. Dc current and current fluctuations are converted to voltages by a low-noise amplifier and are recorded by a computer-controlled data acquisition (DAQ) board. (b) Atomic force microscope image of a representative sample (scale bar: 1 μm). The distance between the electrodes is 300 nm. CNT height is measured as <2 nm. The electrodes are cobalt and niobium, as indicated on the image. (c) Resistance as a function of temperature of a section of the niobium electrode. Transition temperature occurs at 6.5 K.

a)Electronic mail: nina@pha.jhu.edu.

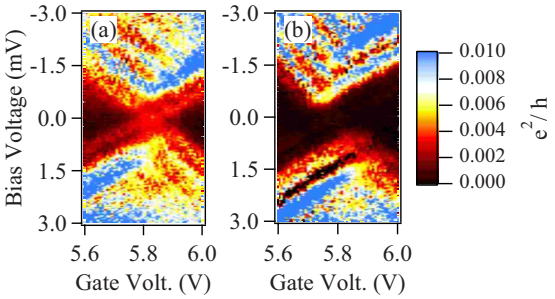

FIG. 2. (Color online) Differential conductance, $G=dI/dV$, for varying gate and bias voltages. Scale bar gives conductance values from a minimum of zero up to a maximum of 0.01 e^2/h. Temperature during measurement is (a) 10 and (b) 4.2 K.

superconducting energy gap mentioned previously is also visible here for the measurements done at 4.2 K.

In Figs. 3(c) and 3(d) we plot the conductance as a function of gate voltage at 10 and 4.2 K, respectively. The measurements at 4.2 K are made at a slightly higher bias to compensate for the superconducting gap. Positive-bias data have been scaled by a factor of 1.2 to compensate for the natural asymmetries in the conductance due to either bias offset or asymmetric electrode couplings. The difference between the positive and negative bias conductances is observed to peak for gate voltages where the normal-metal lead is resonant with an energy level on the dot. The data have been fit using a standard line shape model[31] with the single-junction resonance locations in the gate voltage and the maximum tunneling rates of the junctions as the fitting parameters.

The single-junction conductances used to fit the overall conductance trace at 4.2 K are given in Fig. 4(a). Positive

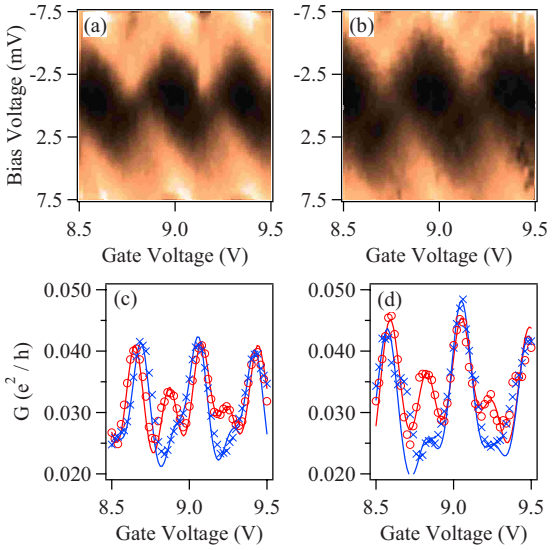

FIG. 3. (Color online) [(a) and (b)] Differential conductance, $G=dI/dV$, for varying gate and bias voltages. Conductance values range from zero (black) up to 0.06 e^2/h (white). Temperature during measurement is (a) 10 and (b) 4.2 K. (c) Conductance as a function of gate voltage at ±5 mV and 10 K for negative (open circle) and positive (crosses) bias. Positive-bias data have been scaled by a factor of 1.2 and shifted in the gate voltage (~0.2 V) to line up conductance peaks. (d) Conductance as a function of gate voltage at ±5.5 mV and 4.2 K for negative (open circle) and positive (crosses). Positive-bias data have been scaled and shifted by the same amounts as (c).

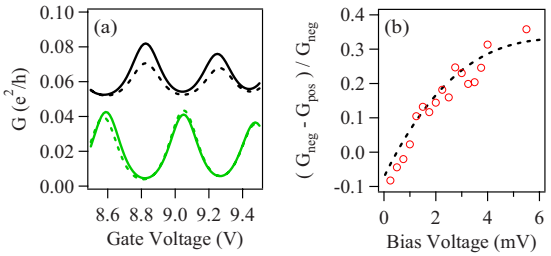

FIG. 4. (Color online) (a) Single-junction conductance as a function of gate voltage. Normal-metal conductance is approximately the same for positive (dashed bottom trace) and negative (solid bottom trace) bias. Ferromagnetic single-junction conductance is shifted by 0.05 e^2/h for readability. Positive-bias (dashed top trace) conductance is lower than negative bias (solid top trace) at the gate voltages $Vg=8.85$ and 9.25 V. (b) Percent difference between positive and negative bias ferromagnetic single-junction conductance as a function of bias voltage. Data (open circles) is taken at a fixed gate voltage of 8.85 V. A guide for the eye is given as a dashed black line.

and negative bias conductances are plotted for both the ferromagnetic and normal-metal tunnel junctions. We observe that the normal-metal single-junction conductance is symmetric with respect to bias direction, while the ferromagnetic single junction is not. It has been proposed[13] that this asymmetry is the result of spin accumulation on the dot. The decrease in the tunneling probability through the ferromagnetic tunnel junction leads to the spin diode effect—the current becomes spin polarized for one direction of the bias. We observe the spin diode effect at both temperatures, provided we compensate for the superconducting gap.

In Fig. 4(b) we plot the percent difference between the positive and negative conductance as a function of the bias voltage. It is seen that the difference decreases toward zero as the bias voltage decreases. This means that the spin diode effect is suppressed for low bias voltages as the coulomb blockade essentially overwhelms all other interactions.

A representative plot of the current noise, S, as a function of frequency for several bias voltages is given in Fig. 5(a) for a fixed gate voltage. These noise measurements were made by sampling the fluctuation of the current at 100 kHz using two low-noise amplifiers. The data from the two amplifiers were cross correlated to reduce amplifier noise.[32] The final noise power was obtained by dividing the power spectral density of the current fluctuations by the white noise response of the system.[33] For low frequencies we see that $1/f$ noise dominates,[34] while for frequencies above ~20 kHz we observe the frequency-independent noise, S_I, which is characteristic of the shot noise.[35]

The shot noise, S_I, is plotted against the current in Fig. 5(b) for one gate voltage. We observe that the noise is proportional to the mean value of the current over a range of the bias voltage. We compute the Fano factor,[36] F, such that $F=S_I/2eI$, where e is the electron charge and I is the mean current for a given gate and bias voltage. Even though the noise is seen to be asymmetric in Fig. 5(b), this asymmetry is primarily due to the nature of the quantum dot. It is well known that the noise is determined by the tunneling rates of the individual junctions,[37] and so depends strongly on the gate voltage.

A plot of S_I as a function of the gate voltage for ±5 mV bias is given in Fig. 5(c). The theoretical value of the Fano

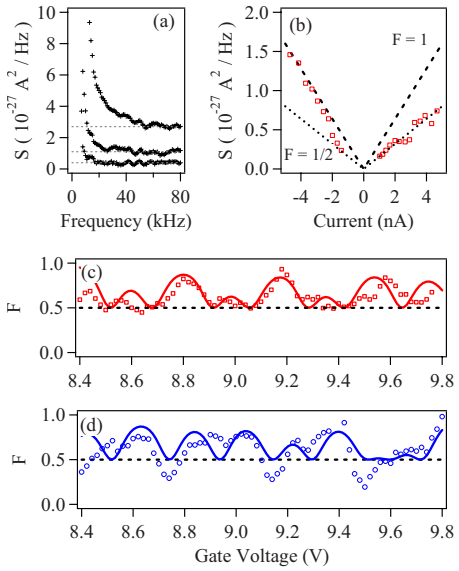

FIG. 5. (Color online) (a) Plot of current noise vs frequency for varying values of bias voltage. Dashed lines are fits to white noise component above ~20 kHz. (b) Representative plot of shot noise vs current for a fixed gate voltage. Data (open squares) are plotted alongside theoretical Fano factor values (dashed lines), $F=0.5$ and $F=1.0$. The size of the squares represents the error bars of the measured Fano factor values. (c) Fano factor data vs gate voltage (open squares) and the theoretical fit based on the conductance data (solid line) for positive bias. Positive-bias values have been shifted in the gate voltage (~0.2 V) to match resonance peaks. (d) Fano factor data vs gate voltage (open squares) and the theoretical fit based on the conductance data (solid line) for negative bias.

factor has been computed[37] according to the conductance data using $F=(\Gamma_L^2+\Gamma_R^2)/(\Gamma_L+\Gamma_R)^2$. For positive bias, we see that the theoretical value for F matches the theory. For negative bias, we observe that the noise dips well below the minimum value of $F=0.5$ for certain values of the gate voltage.

In Fig. 6 we plot the noise dips below the minimum value of $F=0.5$ as a function of the gate voltage. The average value for the minima of the noise dips is measured to be $F=0.28\pm0.07$. Also plotted (right-hand axis) is the current as a function of the gate voltage. We find that the minima of F occur at the gate voltages for which the current reaches a maximum. Values of F below 0.5 are not expected under the standard model for the shot noise.[38] It has been suggested that due to spin-flip events on the dot, the Fano factor could be reduced below the $F=0.5$ limit.[13,39] However, including spin-flip events still does not seem to yield low enough values of F to explain our result. The predicted values are based on the polarization of the cobalt electrode and the absence of polarization in the normal electrode. It is possible that there is an "effective polarization" which is different than expected due to the spin-flip processes. Further study on different systems would be needed to resolve these questions.

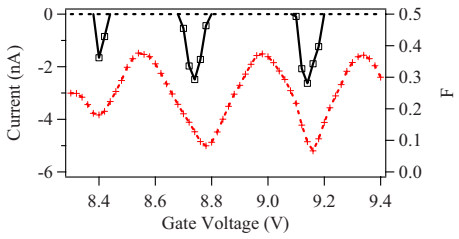

FIG. 6. (Color online) Fano factor dips below $F=0.5$ as a function of gate voltage. Fano factor values (open squares and solid line) are labeled on the right axis. Current (crosses and dashed line) is plotted as a function of gate voltage and labeled on the left axis. Fano factor dips and current maxima occur at the same gate voltages $Vg=8.75$ and 9.15 V. The size of the squares represents the size of the error bars.

It should also be pointed out that super-Poissonian noise might be expected as a result of both spin[13,18,39] and charge[40] accumulation. We find no evidence of this from Fig. 5(c). The predictions of super-Poissonian noise, however, depend largely on bias and gate voltages, as well as on the spin relaxation times, and it is possible that our samples are not in the right regime to observe this.

In conclusion, we have demonstrated a carbon nanotube-based spin diode. With appropriate tuning of the gate and bias voltages, we are able to turn the spin diode effect on or off. We observe that the effect is highest when a single energy level on the dot is near the Fermi level of the normal electrode. The effect is reduced at low bias where the Coulomb blockade effect dominates. We have also seen a significant periodic reduction in the current shot noise, which may be due to increased spin-flip rates at certain gate voltages.

We thank J.C. Egues for useful comments. This work was supported in part by the National Science Foundation under Grant Nos. ECCS-0403964, DMR-0547834 (CAREER), and DMR-0520491 (MRSEC), Alfred P. Sloan Foundation under Grant No. BR-4380, and ACS PRF # 42952-G10.

[1] S. Iijima, Nature (London) **354**, 56 (1991).
[2] R. Saito, G. Dresselhaus, and M. S. Dresselhaus, *Physical Properties of Carbon Nanotubes* (Imperial College, London, 1998).
[3] A. Naeemi, R. Savari, and J. D. Meindl, IEEE Electron Device Lett. **26**, 84 (2005).
[4] J. R. Kim, H. M. So, J. Kim, and J. J. Kim, Phys. Rev. B **66**, 233401 (2002).
[5] S. Chakraborty, K. M. Walsh, B. W. Alphenaar, L. Liu, and K. Tsukagoshi, Appl. Phys. Lett. **83**, 1008 (2003).
[6] A. Jensen, J. R. Hauptmann, J. Naygard, and P. E. Lindelof, Phys. Rev. B **72**, 035419 (2005).
[7] S. Sahoo, T. Kontos, J. Furer, C. Hoffmann, M. Graber, A. Cottet, and C. Schonenberger, Nat. Phys. **1**, 99 (2005).
[8] M. Bockrath, D. H. Cobden, P. L. McEuen, N. G. Chopra, A. Zettl, A. Thess, and R. E. Smalley, Science **275**, 1922 (1997).
[9] M. J. Biercuk, D. J. Reilly, T. M. Buehler, V. C. Chan, J. M. Chow, R. G. Clark, and C. M. Marcus, Phys. Rev. B **73**, 201402 (2006).
[10] D. S. Saraga, G. Burkard, J. C. Egues, H. A. Engel, P. Recher, and D. Loss, Turk. J. Phys. **27**, 427 (2003).
[11] V. Bouchiat, N. Chtchelkatchev, D. Feinberg, G. B. Lesovik, T. Martin, and J. Torres, Nanotechnology **14**, 77 (2003).
[12] I. Weymann and J. Barnas, Appl. Phys. Lett. **92**, 103127 (2008).
[13] F. M. Souza, J. C. Egues, and A. P. Jauho, Phys. Rev. B **75**, 165303 (2007).
[14] H. Dalgleish and G. Kirczenow, Phys. Rev. B **73**, 235436 (2006).
[15] A. A. Shokri, M. Mardaani, and K. Esfarjani, Physica E (Amsterdam) **27**, 325 (2005).
[16] P. Recher, E. V. Sukhorukov, and D. Loss, Phys. Rev. Lett. **85**, 1962 (2000).
[17] R. Świrkowicz, J. Barnaś, M. Wilczyński, W. Rudziński, and V. K. Dugaev, J. Magn. Magn. Mater. **272–276**, 1959 (2004).
[18] B. R. Bulka, Phys. Rev. B **62**, 1186 (2000).
[19] C. A. Merchant and N. Markovic, Phys. Rev. Lett. **100**, 156601 (2008).
[20] C. Beenakker and C. Schonenberger, Phys. Today **56**(5), 37 (2003).
[21] P. Barthold, F. Hohls, N. Maire, K. Pierz, and R. J. Huang, Phys. Status Solidi C **3**, 3786 (2006).
[22] O. Zarchin, Y. C. Chung, M. Heiblum, D. Rohrlich, and V. Umansky,

Phys. Rev. Lett. **98**, 066801 (2007).
[23]H. Birk, M. J. M. de Jong, and C. Schonenberger, Phys. Rev. Lett. **75**, 1610 (1995).
[24]J. Kong, H. T. Soh, A. M. Cassell, C. F. Quate, and H. Dai, Nature (London) **395**, 878 (1998).
[25]D. V. Averin and K. K. Likharev, J. Low Temp. Phys. **62**, 345 (1986).
[26]H. Grabert and M. H. Devoret, *Single Charge Tunneling* (Plenum, New York, 1992).
[27]M. Tinkham, *Introduction to Superconductivity* (McGraw-Hill, New York, 1995).
[28]M. R. Graber, T. Nussbaumer, W. Belzig, and C. Schonenberger, Nanotechnology **15**, S479 (2004).
[29]J. A. van Dam, Y. V. Nazarov, E. P. A. M. Bakkers, S. De Franceschi, and L. P. Kouwenhoven, Nature (London) **442**, 667 (2006).
[30]D. H. Cobden and J. Nygard, Phys. Rev. Lett. **89**, 046803 (2002).
[31]C. Beenakker, Phys. Rev. B **44**, 1646 (1991).
[32]M. Sampietro, L. Fasoli, and G. Ferrari, Rev. Sci. Instrum. **70**, 2520 (1999).
[33]F. Liefrink, J. I. Dijkhuis, M. J. M. de Jong, L. W. Molenkamp, and H. van Houten, Phys. Rev. B **49**, 14066 (1994).
[34]Y. P. Li, D. C. Tsui, J. J. Heremans, and J. A. Simmons, Appl. Phys. Lett. **57**, 774 (1990).
[35]A. Nauen, F. Hohls, N. Maire, K. Pierz, and R. J. Huang, Phys. Rev. B **70**, 033305 (2004).
[36]U. Fano, Phys. Rev. **72**, 26 (1947).
[37]A. Thielmann, M. H. Hettler, J. Konig, and G. Schon, Phys. Rev. B **68**, 115105 (2003).
[38]Y. M. Blanter and M. Buttiker, Semicond. Sci. Technol. **19**, 663 (2004).
[39]I. Djuric, B. Dong, and H.-L. Cui, IEEE Trans. Nanotechnol. **4**, 71 (2005).
[40]V. H. Nguyen and V. L. Nguyen, Phys. Rev. B **73**, 165327 (2006).